



Article

Investigation of LCD 3D Printing of Carbon Fiber Composites by Utilising Central Composite Design

Raveen Mohammed Salih ^{1,*}, Abdulkader Kadauw ^{1,2}, Henning Zeidler ² and Rezo Aliyev ²

¹ Mechanical and Mechatronic Engineering Department, College of Engineering, Salahaddin University Erbil, Erbil 44001, Iraq

² Institute for Machine Elements, Engineering Design and Manufacturing, TU Bergakademie Freiberg, 09599 Freiberg, Germany

* Correspondence: ravin.rizgar@gmail.com

Abstract: The technology of additive manufacturing (AM) has transformed the fields of machinery, aerospace, and electronics. Adopting cost-effective, precise, and rapid procedures in AM is one of the major concerns of today's industry. Stereolithography is a promising AM technique that is thought to meet these requirements. However, the fact that materials printed with stereolithography do not have good mechanical properties limits their application, such as in biomedicine and aerospace. Previous studies have shown the shortcomings of stereolithography printers. This research focuses on enhancing the mechanical characteristics of the polymer resin used in stereolithography (SLA)-like liquid crystal display (LCD) 3D printers by fabricating a new AM composite material with carbon fibers. For this reason, chopped carbon fibers (0.1 mm size) at amounts of 0.25 wt% and 0.5 wt% have been used with Acrylonitrile butadiene styrene (ABS)-like photopolymer transparent resin during the printing process, and three different print layer thicknesses were tested. For the design of the experiment (DoE), Q-DAS software was used to analyze the resulting data. A tensile-testing machine was utilized to determine the ultimate strength using the ASTM D638 standard. The results show an increase in the ultimate strength by adding carbon fiber to some extent, but after a certain percentage of carbon fiber added, the strength drops off.

Keywords: stereolithography (SLA); LCD; DLP; carbon fiber; Q-DAS; composite material; resin; ABS-like photopolymer; design of the experiment (DoE)



Citation: Salih, R.M.; Kadauw, A.; Zeidler, H.; Aliyev, R. Investigation of LCD 3D Printing of Carbon Fiber Composites by Utilising Central Composite Design. *J. Manuf. Mater. Process.* **2023**, *7*, 58. <https://doi.org/10.3390/jmmp7020058>

Academic Editor: Jing Shi

Received: 27 January 2023

Revised: 22 February 2023

Accepted: 24 February 2023

Published: 4 March 2023



Copyright: © 2023 by the authors. Licensee MDPI, Basel, Switzerland. This article is an open access article distributed under the terms and conditions of the Creative Commons Attribution (CC BY) license (<https://creativecommons.org/licenses/by/4.0/>).

1. Introduction

It is believed that 3D printing would revolutionize the entire product design process as a production approach [1,2]. The layering method of making things replaces the requirement for costly molds and makes it possible to produce highly optimized and geometrically complicated structures. It is perfect for low-volume manufacturing such as prototyping, customization at scale, and print-based-on-demand. It can also help streamline the logistics of the supply chain in the direction of distributed manufacturing at local sites, using new 3D printing materials, such as polymers, metals, ceramics, and electronics. There are currently numerous types of additive manufacturing processes, such as stereolithography (SLA), fused filament fabrication (FFF), selective laser sintering, and inkjet printing [3,4]. These additive manufacturing processes enable the production of intricate products that cannot be accomplished with conventional machining techniques, and they are employed in a range of industries, including the mechanical, aerospace, and electronic sectors. Using a 3D printer, objects that were previously assembled from several components can now be created in a single step [5]. It is anticipated that 3D printing would make it possible for medical and assistive technology businesses to manufacture individualized prosthetics and artificial bones. Additionally, the aerospace industry has a significant demand for precision components that come in a wide variety of shapes. However, the 3D printing materials that

are used does not help due to their properties. You can have the best printer in the world, but the quality of the product depends on the material with which you choose to print. When you realise that you can now print in 3D for structural or biomedical applications, the relevance of printing quality becomes clear. Polymer was the well-known material of the 20th century due to its ability to deliver economic and structural benefits; nevertheless, from the standpoint of 3D printing, the lack of mechanical strength and functionality is a major obstacle for their widespread usage [6]. In order to increase the mechanical, thermal, and durability properties, the composites might be called the reference materials of the twenty-first century [7] if many materials are combined to address these issues. The next frontier is the development of novel composite materials that are compatible with existing printers and capable of meeting the requirements of specialized applications [8–11]. When it comes to the resin that is commonly used in 3D printers, it has poor mechanical properties [12–14]. Resin 3D printers have historically been costly and unwieldy, requiring specialised technicians and costly service contracts. Today's small-format desktop printers produce industrial-grade output at significantly lower costs and with unmatched versatility. Stereolithography is a method of the additive manufacturing technology referred to as vat photopolymerization or resin 3D printing. All of these devices utilize a light source, such as a laser or projector, to turn liquid resin into solid plastic. The arrangement of the important components, such as the light source, the build platform, and the resin tank, is the most distinguishing physical characteristic of these devices [15–17].

The resin is utilized most commonly in the production of prototypes in addition to toys because it is not suited for the production of functioning structures. The quality and resolution of 3D-printed resin objects can be higher than their FFF counterparts, but they are often weaker. This is partially owing to the nature of the substance, as well as the polymerization process, which does not always produce strong bonds. Most conventional resins are very brittle compared to other 3D-printing materials and are unsuitable for stressed parts or outdoor use; thus, researchers are attempting to enhance the mechanical characteristics of resin printing by applying a variety of reinforcing techniques [18,19]. Methods that utilize mixtures of thermoplastic filaments and granules or short fibers, such as carbon black or reinforcing platelets, chopped carbon fibers, polymer fibrils, carbon nanotube (CNT), and glass fibers, are currently being evaluated. Additionally, methods that utilize continuous fibers infused with thermoplastic filaments are also being considered. In contrast, FFF utilizes a technique called lamination in order to mix many layers of a thermoplastic material. Delamination and premature failure are potential outcomes of this technique [20–22]. As a result of the minimal laminated layer thickness of 0.1 mm, the fabrication precision is unsatisfactory, and there are concerns regarding structural elements such as large voids between filaments. Another challenge is the distortion that occurs as a result of the heat-shrinkability of the resin. Popularity has increased for SLA 3D printers as a partial solution to these problems. As heat shrinkage is practically nonexistent in SLA, the laminate layers are thin and the fabrication precision is outstanding. SLA-based 3D-printing techniques include projector printing, rubber material printing, and nanostructure printing. Due to the limited mechanical capabilities of the SLA resin, reinforcements are necessary to produce components with high mechanical properties. Numerous studies have been conducted on manufacturing methods utilizing cellulose nanocrystals, graphene oxide, or SiO₂. However, their mechanical properties show weaker results to those of composites manufactured using traditional procedures and based on continuous fibers [23–29].

Moreover, to fulfil specific tasks other than mechanical behaviour, numerous 3D-printed materials such as CNT or graphene-based materials with added electrical functionality have been created. Ref. [30] conducted research on SLA-printed nonwoven glass fiber mat/epoxy composites. However, they utilised a single layer of fabric for the additive manufacturing process. To increase the mechanical qualities of SLA-printed objects, reinforcement is necessary in the form of many layers of continuous fibers. Some research discusses the usage of filaments comprised of a thermoplastic matrix including short strands. Examples of fiber materials are continuous or short carbon fiber (CF), Kevlar,

carbon nanotubes (CNTs), alumina, kenaf, glass, and natural fibers such as bamboo [31]. The load-bearing capability of acrylonitrile butadiene styrene (ABS) was enhanced by combining it with short carbon fibers (3.2 mm in length) for 13 min at 220 °C in a compounder with a rotor speed of 60 revolutions per minute. The substance was then used to produce filament, and samples were printed using a desktop printer. ABS with 30 wt% CF showed a 77% increase in tensile strength (from 35 MPa to 62 MPa) in comparison to ABS without CF. Moreover, attempts to create 40 wt% CF were made; however, the extrusion nozzle constantly clogged, limiting the number of printed layers [32]. Carbon-fiber-reinforced polymer (CFRP) filament was produced by mixing ABS plastic pellets and CF powders (powder diameter: 130 μm and 100 μm) at a temperature of 220 °C. The addition of 5% CF increased the tensile yield strength of specimens produced by a home printer by 25% (from 34 MPa to 42 MPa). There was an attempt to obtain greater CF loadings, but porosity harmed the samples to the extent that their tensile strength was lower than that of the 5 wt% specimens. Studying the 3D printing of a UV-curable resin reinforced with continuous carbon fibers revealed that the composite structures had superior mechanical performance and excellent thermal stability due to the crosslinked nature of the material and higher load-bearing capacity, due to the dispersion of continuous carbon fiber throughout the polymer matrix [33]. Due to the underlying principles of stereolithography 3D printing, however, reinforcing polymer material with continuous fiber remains difficult. Using short fibers to 3D-print thermoset composites by photopolymerization is therefore more prevalent, as the use of continuous fibers for thermoset resin 3D printing is still relatively novel [34]. Moreover, the shear alignment of the short fiber has been studied. Shear alignment is generated by the movement of the vat in relation to the build plate. Better fiber alignment in the 3D-printing matrix material can lead to superior mechanical performance; in this example, the flexural characteristics of SLA-printed composites increased by 90% compared to randomly distributed samples [35]. A quality composite 3D printer should meet a number of prerequisites. It should (1) be able to build complex, detailed, and durable parts; (2) enable users to control the attributes of the composite structures by freely aligning the fibers and varying the compositions; and (3) have high precision for improved reproducibility. Due to the limited investment in this area and the technical challenges, these prerequisites have not been reached [36,37].

In this study, the SLA-related Liquid Crystal Display (LCD) was employed to evaluate a photopolymer resin mixed with 100 μm carbon fiber powder, utilizing a bottom-up LCD photopolymerization platform. Carbon contents of 0.25 wt% and 0.5 wt% were used with print layer thicknesses of 30 μm , 40 μm , and 50 μm . ABS-like photopolymer resin, which is readily available, was chosen as the fiber-free resin. The ABS-like photopolymer resin has a liquid density of 1.100 g/cm³, a solid density of 1.195 g/cm³, solidification wavelengths around 405 nm, and a viscosity (at 25 °C) between 150–200 mPa·s. The investigation focuses on finding the reasons behind the results through studying the microstructure of the samples.

2. Material and Methods

2.1. Carbon Fiber

Milled carbon fiber is a black filler powder composed of finely crushed carbon fibers. To increase tensile strength, dimensional stability, and electrical conductivity, it can be added to tooling resins, casting resins, thermoplastics, adhesives, coating, and paints [38,39]. In this paper, milled carbon fiber was used to reinforce the 3D printing resin and its influences on the mechanical characteristics of the newly formed composite material (milled carbon fiber + photopolymer resin) was tested. The milled carbon used is made from recycled fibers. The carbon fibers used therefore are equipped largely with PU-sizing. The majority of the sizing evaporates during milling due to the heat produced. When dry, the milled fibers form fiber balls that dissolve and spread out evenly in resin. Manufactured by R&G Faserverbundwerkstoffe GmbH (Waldenbuch, Germany), the density of the material at 20 °C is between 1.7–2.0 g/cm³, with carbon content of 94% and Monofilament diameter

of $7 \mu\text{m} \pm 2$, The size of the milled carbon fiber used in this study was $100 \mu\text{m}$ as shown in Figure 1, and it was tested with the resin in two different amounts (0.25 wt% and 0.5 wt%).



Figure 1. Milled carbon fiber, $100 \mu\text{m}$.

2.2. ABS-like Photopolymer Resin

The material used in this study is ELEGOO ABS-like photopolymer resin. This material is a type of polymer whose physical characteristics change when exposed to light; it is also volatile-organic-compound-free. In the context of additive manufacturing, this is a typical liquid plastic resin that solidifies when exposed to a light source, such as a laser, a lamp, a projector, or light-emitting diodes (LEDs), with the majority of these light sources emitting ultraviolet (UV) light, which is compatible with our photo-curing resin. The print quality is excellent in terms of detail and performance, making it an ideal companion for LCD 3D printers. Included among the properties of ELEGOO photopolymer resin are the following: (1) Low shrinkage and exactness: The ELEGOO photopolymer resin is developed to reduce volume shrinkage during the photo-curing process, hence ensuring the high precision and smooth finish of the printed model. (2) Rapid curing and excellent stability of ELEGOO 405 nm rapid resin was designed to effectively minimize printing time. In addition to great stability and appropriate hardness, it ensures a worry-free printing experience and successful printing. (3) Extensive range of uses: ELEGOO photopolymer resin is compatible with DLP and LCD 3D printers that use ultraviolet light to cure models. It has numerous applications, ranging from miniatures for board games to industrial parts and components. It is also used to print 3D CAD designs and bring them from concept to reality [40]. The ABS-like photopolymer resin shown in Figure 2 has a liquid density of 1.100 g/cm^3 and a solid density of 1.195 g/cm^3 , solidification wavelengths around 405 nm, and a viscosity (at $25 \text{ }^\circ\text{C}$) between 150 and 200 mPa·s.



Figure 2. ABS-like photopolymer resin used in the study.

2.3. Stereolithographic 3D Printing

This research utilises an ELEGOO Mars LCD printer. The XY resolution of a 2560×1440 2K LCD panel supported by an array of 405 nm UV lights and mirrors is 0.047 mm, which is the industry standard. With a minimum layer height of 0.01 mm, the Mars is able to pro-

duce prints of substantially greater quality than even the most sophisticated FFF printers. Figure 3 shows the ELEGOO Mars printer used in the study. In the investigation, CHITUBOX slicing software was employed with the ELEGOO Mars printer to slice the tensile sample design. The printer's 3.5-inch colour touch display makes off-line printing simple. ELEGOO Mars employs a 2560×1440 2K HD masking LCD to deliver precise printing with XY axis resolution of 0.047 mm, Z axis accuracy of 0.00125 mm, layer thickness range of 0.01–0.2 mm, printing speed of 22.5 mm/h, a build volume of $4.72 \times 2.68 \times 6.1$ inches, and a power need of 110–220 V.



Figure 3. ELEGOO Mars printer used in the study.

Resin 3D printers mostly utilize three printing technologies, SLA, DLP, and LCD, all of which share a similar operating procedure and applications (Figure 4).

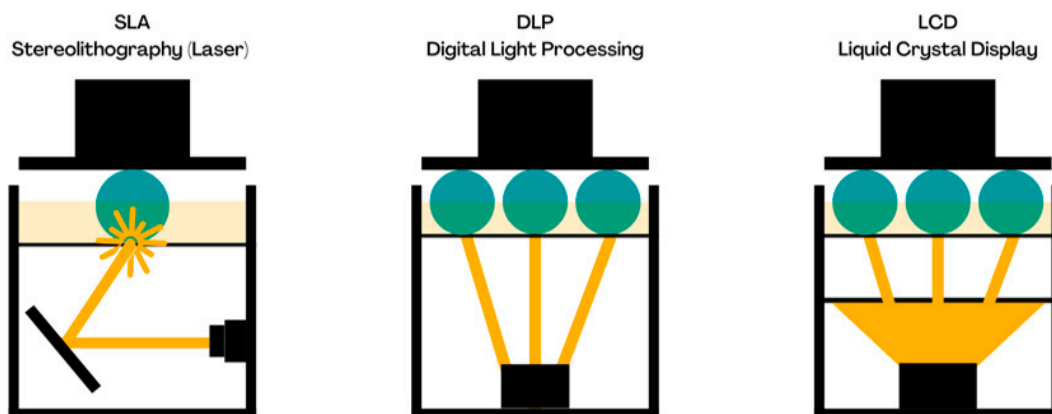


Figure 4. Schematic diagram of the different types of resin printing: SLA, DLP, LCD [41].

SLA is a sort of additive manufacturing technology that uses a high-powered laser as the light source to harden a photosensitive liquid, layer by layer, in a photochemical process in which 3D models are gradually created and generated across a defined area. Digital light processing (DLP) employs a digital light projector rather than a laser to concurrently cure all portions of the resin. DLP 3D printers can construct a 3D model more quickly than SLA printers because each layer solidifies more rapidly. An array of flat UV LCD panels projects light directly onto the build platform in LCD 3D printers. LCD light density is the

most crucial factor in making high-quality printouts. LCD light with a higher resolution produces greater print quality [41–43].

2.4. Specimen Manufacturing

We used the ELEGOO Mars LCD 3D printer to manufacture specimens for the present study. By applying ASTM D638 standard, specimens were built in the 3-dimensional CAD software called Solidworks 2019 and transformed to STL format. The CHITUBOX slicing software was utilized to slice the layers and regulate other parameters, such as the 405 nm wavelength. First layer exposure time was 70 s, normal exposure time was 12 s, and layer thicknesses were 0.3, 0.4, and 0.5 mm. Initially, specimens were printed without carbon fiber using only translucent resin (Figure 5A). Before printing, carbon fibers were introduced randomly to an ABS-like photopolymer resin and manually mixed for 60 s (Figure 5B). The test specimens were produced by curing for 10 min in an exposure unit following the completion of manufacturing. In this investigation, several carbon percentages were evaluated, and for each control factor, three specimens were printed to ensure the correctness of the test results. Figure 6 depicts a schematic of the production of the specimen, including carbon fibers, using the LCD machine [44–46].

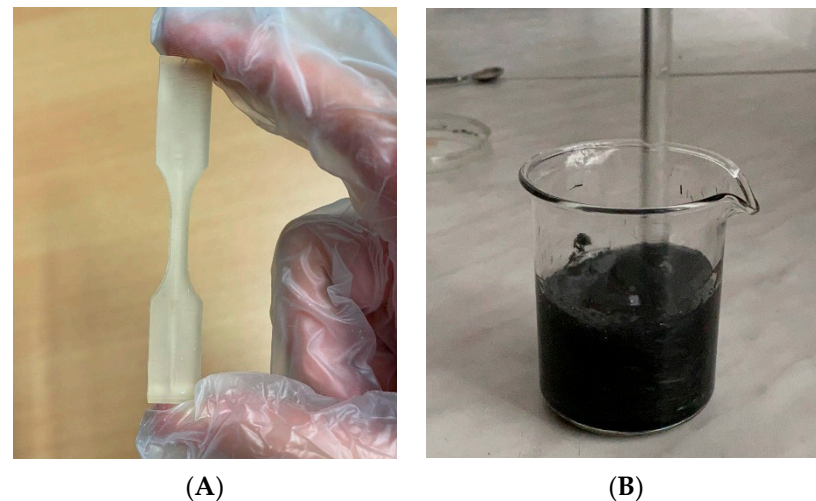


Figure 5. (A) 3D-printed specimen with 0 wt% carbon; (B) carbon fiber and photopolymer resin during manual blending.

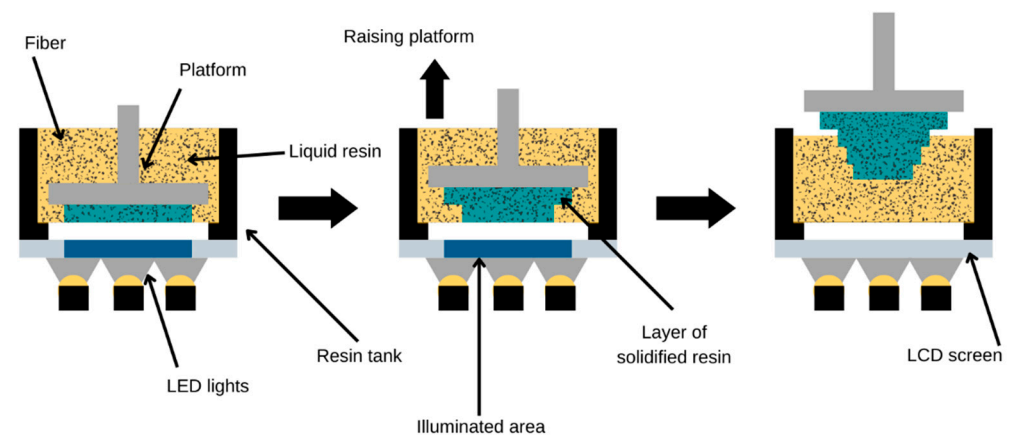


Figure 6. Schematic diagram of the 3D-printing composite using LCD resin printing, Reprinted/adapted with permission from Ref. [44] 2018, Sano, Y.; Matsuzaki, R.; Ueda, M.; Todoroki, A.; Hirano, Y.

2.5. Design of Experiments (DoE) Using Q-DAS

Design of experiments (DoE) is a technique that permits scientists and engineers to efficiently and systematically investigate the relationship between various input variables

(also known as factors) and important output variables (also known as responses) [45]. It is a technique for collecting and analyzing data to determine whether a factor or set of factors affects the response. It is also used to determine whether factors influence the response collectively and to optimize the response by simulating the response's behavior as a function of the factors.

There are currently numerous DoE software packages available; Q-DAS version 13 was utilized to analyze the data for this investigation in order to plan and establish project objectives and analyze the relationship between elements influencing the process and its output. These two control factors were chosen each with 3 levels (carbon content and layer thickness) and one resulting factor (tensile testing) shown in Figure 7. Since the study consists of 2 factors on 3 levels, central composite design (CCD) is applied in this study to generate the DoE according to the CCD; the cube points are repeated 2 times and the central point 3 times, which in total sum up to 15 samples.

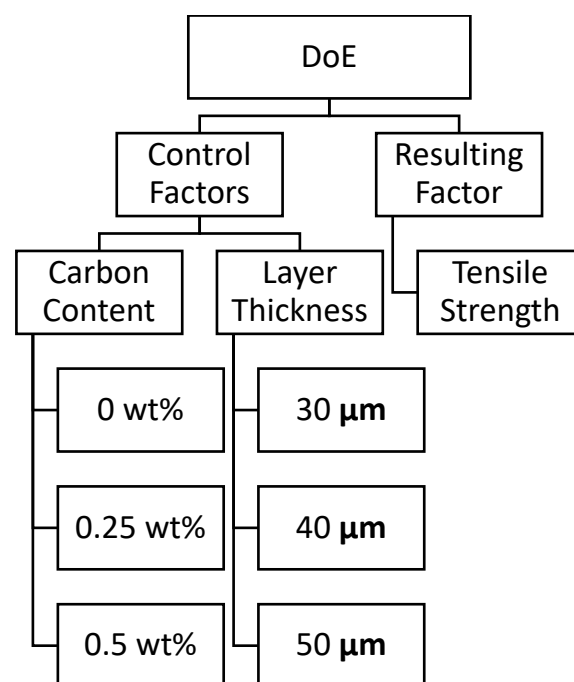


Figure 7. Diagram illustrating the DoE process with the control factors of carbon content using three different carbon % and layer thickness using three different layer thickness values and resulting factor of tensile strength with total of 15 sample according to Q-DAS using central composite design method.

2.6. Mechanical Tests

Tensile tests were performed on the specimen without carbon fiber and carbon fiber specimens. The specimen dimensions were prepared according to the ASTM standard D638 (dimensions as below), as shown in Figure 8A. Three specimens were manufactured for each control factor, as shown in Figure 8B. A Universal Tensile Machine called Inspekt Retrofit AGS-G 10 kN was used (Figure 9). The loading rate used for the tensile testing was 1.00 mm/min [46–48].

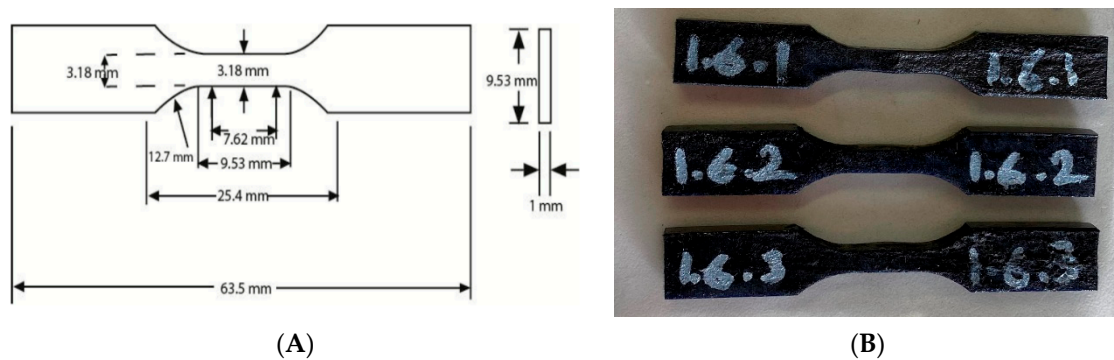


Figure 8. (A) ASTM D638 standard dimension; (B) example of 3 specimens printed for each case.

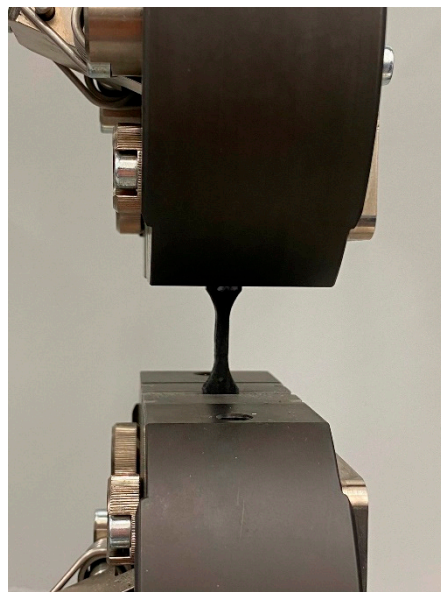


Figure 9. Universal Tensile Machine Inspekt Retrofit AGS-G 10 kN.

3. Results and Discussion

3.1. Composite Material 3D Printing

Based on the analysis of the experimental design data, the ideal number of instances for two control factors with three levels was 15 (Figure 10). Each example was printed and tested three times, resulting in a total of 45 printed specimens. Carbon content (0, 0.25, and 0.5 wt% CF) and layer thickness (30, 40, and 50 μm) were chosen as the most influential control factors after several iterations of modifying different parameters shown in Table 1. A non-uniform distribution of the fiber material was seen in the in-plane direction. This non-uniform distribution of the carbon fiber has an effect on the surface roughness of the specimen. The surface roughness increased according to the amount of carbon fiber added, but the 0.25 wt% had almost no effect. Beginning at 0.50 wt% and above, the dimension and design of the part will be impacted by the surface roughness. During the iteration process, up to 2 wt% CF was used and the results show a very rough surface and some very small voids of <math><1\text{ mm}</math>.



Figure 10. Dog-bone tensile specimens before and after tensile test.

Table 1. Printed specimen data according to DoE iterations.

No.	Carbon Percentage wt%	Layer Thickness μm
1	0.00	30
2	0.50	30
3	0.00	50
4	0.50	50
5	0.00	30
6	0.50	30
7	0.00	50
8	0.50	50
9	0.00	40
10	0.50	40
11	0.25	30
12	0.25	50
13	0.25	40
14	0.25	40
15	0.25	40

3.2. Mechanical Characteristics of the Specimens

The results of the tensile tests vary, depending on the carbon content and layer thickness, with some demonstrating a remarkable improvement in tensile strength and others showing a drop in tensile strength in comparison to the specimen printed without carbon fiber. The resulting tensile strength of all 15 samples is shown in Table 2. The tensile tester was used to construct the force—displacement graph. (Figure 11) depicts the force—displacement graph for a sample printed without carbon fiber and with a layer thickness of 0.03 mm. This sample has a greater displacement than samples printed with carbon fiber, but withstands a lower force. (Figure 12) depicts the force—displacement graph for a sample printed with a 0.03 mm layer thickness and 0.5 wt% carbon fiber, which demonstrates a lower displacement and force than Figure 13, which depicts a sample printed with a 0.03 mm layer thickness and 0.25 wt% carbon fiber, which demonstrates the highest force and a better displacement than 0.5 wt% carbon fiber. The response surface plot (Figure 14), generated in Q-DAS, shows the effect of both carbon percentage and layer thickness on the tensile test results.

Table 2. Tensile test results.

No.	Carbon Fiber Percentage wt%	Layer Thickness μm	Tensile Strength MPa
1	0.00	30	58.96
2	0.50	30	74.98
3	0.00	50	51.29
4	0.50	50	72.42
5	0.00	30	55.72
6	0.50	30	73.57
7	0.00	50	49.76
8	0.50	50	72.20
9	0.00	40	52.10
10	0.50	40	74.20
11	0.25	30	87.16
12	0.25	50	80.32
13	0.25	40	82.27
14	0.25	40	83.40
15	0.25	40	82.54

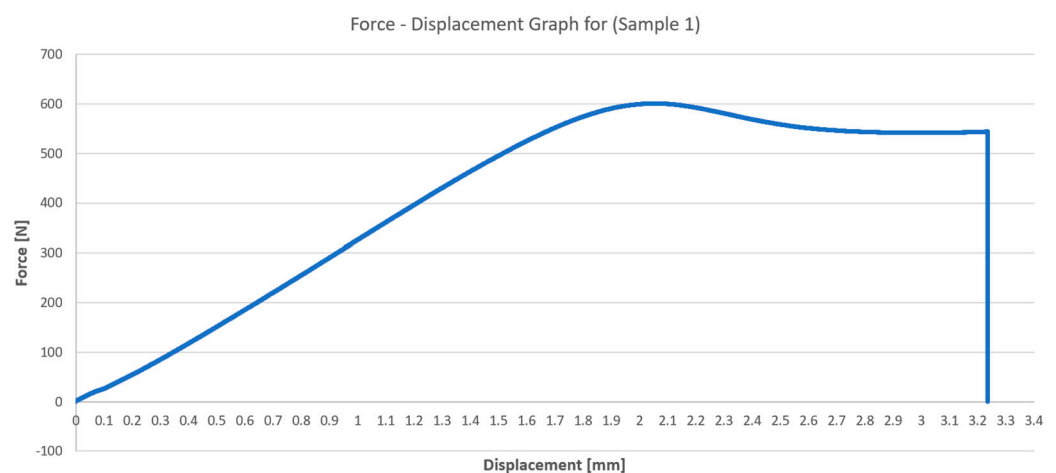


Figure 11. Force—displacement graph for sample 1.

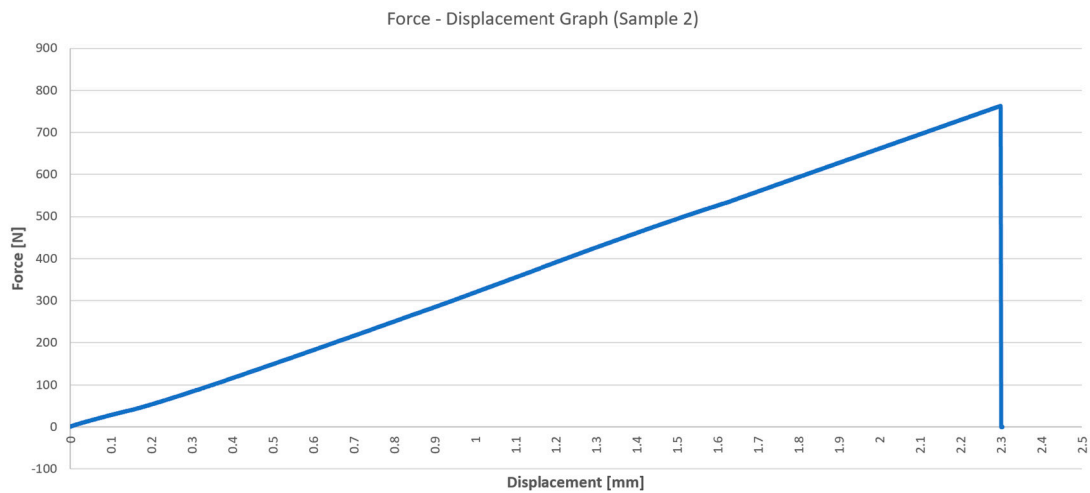


Figure 12. Force—displacement graph for sample 2.

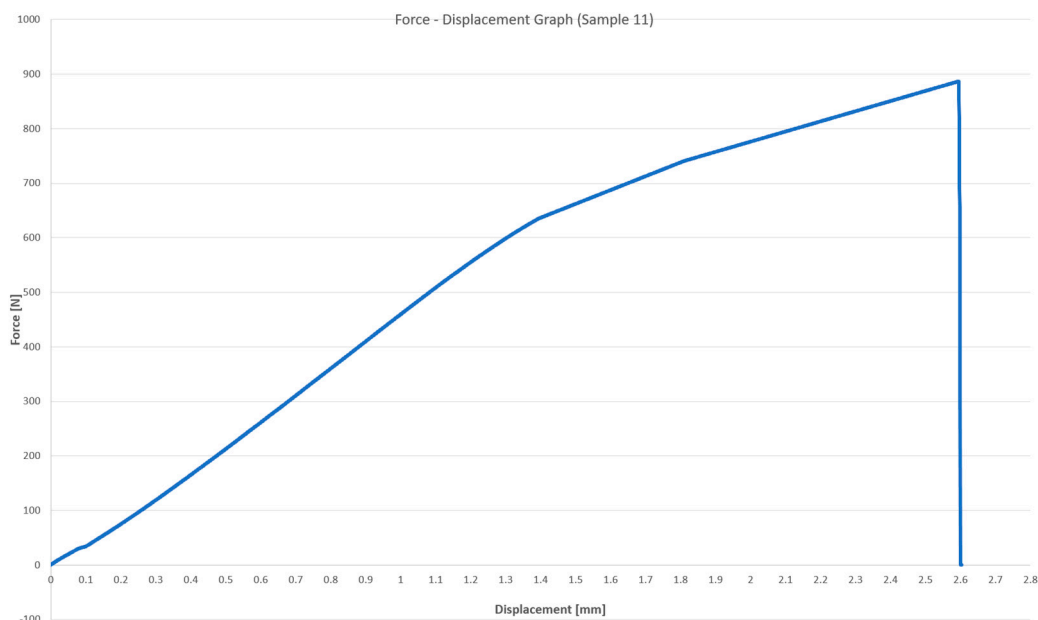


Figure 13. Force—displacement graph for sample 3.

The response plot diagram is used to demonstrate the response of a factor in reaction to a change in other control factors, and it illustrates the changes in a single diagram. As can be seen in the response surface plot, the response depends on two independent factors, in this case, carbon fiber percentage and layer thickness. The highest tensile strength, which is 87.16 MPa, is represented as the dark red color in the response surface plot, and, at that point, the carbon fiber percentage is 0.25 wt% and layer thickness of 30 μm . The result shows a 47.82% increase in tensile strength compared to the specimen printed with the same layer thickness but without carbon fiber. The lowest tensile strength, represented in dark blue, is 49.76 MPa and occurs at 0 wt% carbon fiber and 50 μm layer thickness.

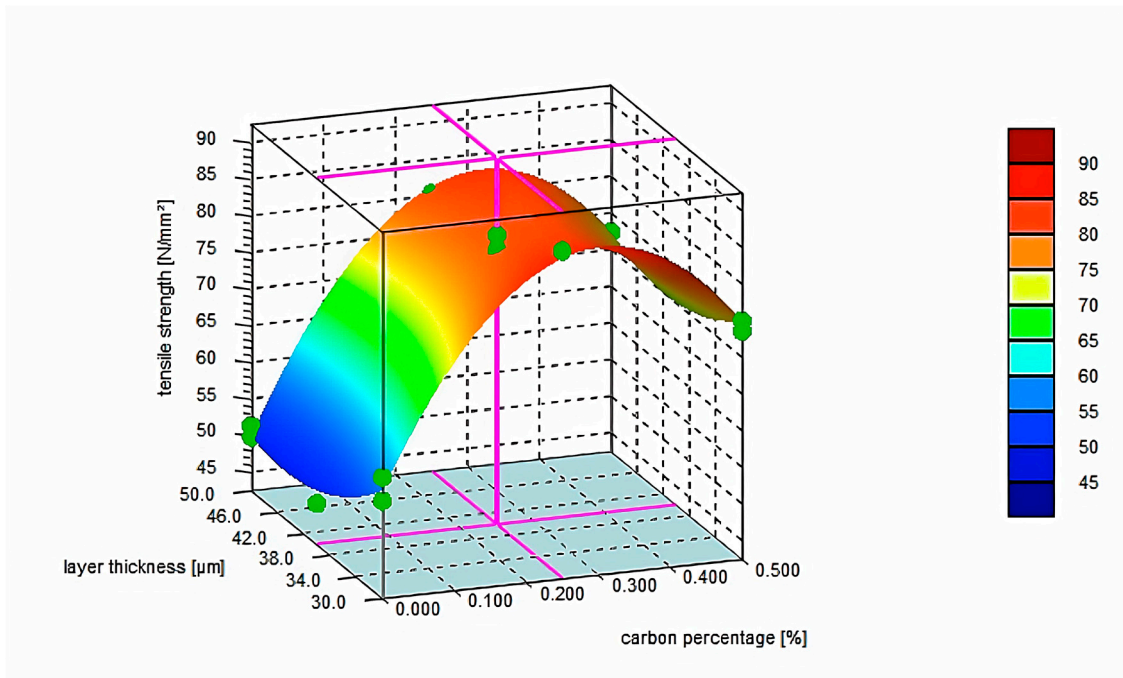


Figure 14. Response surface plot for the two independent control factors and one resulting factor using Q-DAS.

3.2.1. Effect of Carbon Fiber Percentages on the Tensile Test Results

Adding carbon fiber to a certain extent increases the printed part’s tensile strength; however, there is a point at which the strength decreases due to cracks and voids produced by the amount of carbon fiber added. This study demonstrates that a 0.25 wt% to 0.3 wt% of a 100-micrometer carbon fiber size produces the maximum strength with a printing layer thickness of 30 μm (Figure 15); higher carbon fiber content decreases the tensile strength until it becomes weaker than the actual photopolymer resin.

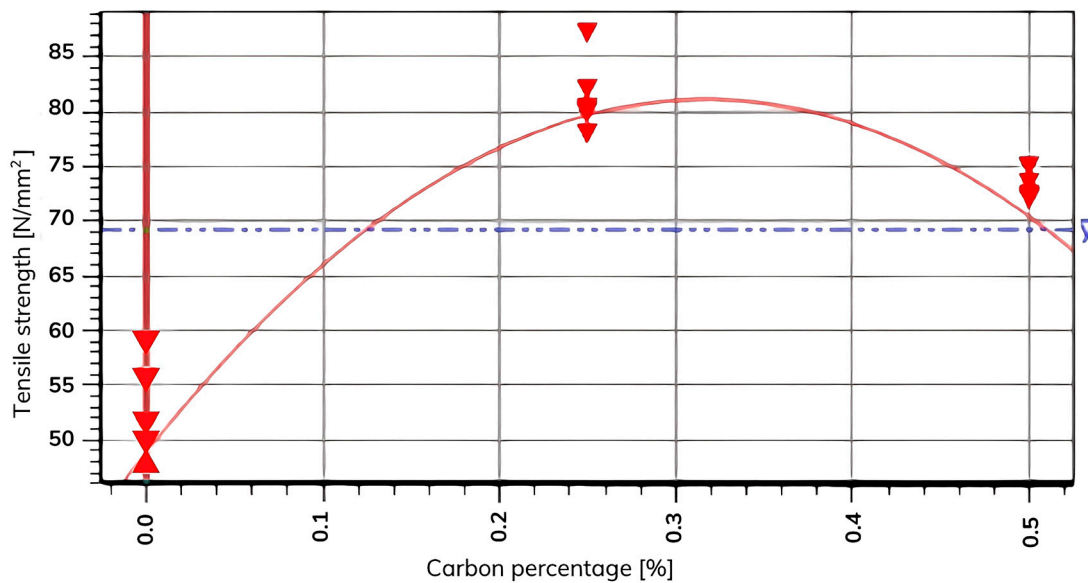


Figure 15. Schematic diagram of carbon fiber percentage and tensile strength showing the effect of carbon percentage on the tensile test results.

3.2.2. Influence of Layer Thickness on the Tensile Strength

The results of the layer thickness when plotted forms a linear graph, meaning that the thinner the printing layer, the higher the tensile strength, whereas increasing the layer thickness will affect the tensile strength negatively. As can be seen in Figure 16, a 30-micrometer layer thickness shows a higher tensile strength compared to a 40- and 50-micrometer layer thickness. However, printing the thinner layer will take longer.

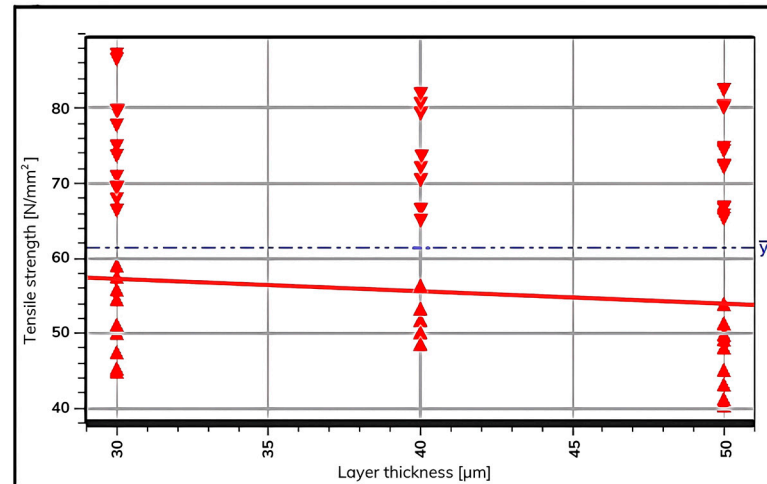


Figure 16. The influence of layer thickness variation on tensile strength.

3.3. Sectional Examination of the Specimens

To examine the distribution of carbon fibers within the specimens, cross-sectional analyses of both 0.25 wt% and 0.5 wt% milled carbon fiber samples were carried out using a scanning electron microscope (SEM; TESCAN MIRA 3). The cross-sections of the specimens containing carbon fiber were analyzed to understand the decrease of tensile strength between the 0.5 wt% compared to the 0.25 wt% carbon fiber. When referring to the carbon fiber specimens, the placement of fibers was skewed toward the bottom; only some fibers could be seen at the top. Due to this, the concentration of the carbon fiber was much higher at the bottom. The reason for the decrease in tensile strength for the 0.5 wt% compared to the lower carbon fiber content is the number of voids and cracks that were generated during the fabrication of the specimen. Figure 17 shows the voids and cracks produced as a result of adding carbon fiber up to 0.5 wt% which, instead of further increasing the tensile strength, causes a decrease.

As an effect of the carbon fiber being distributed throughout the printed layers, a gap is created between the ABS-like photopolymer resin and the carbon fiber during solidification, resulting in a greater number of gaps and cracks in parts of the material. In Figure 18A, small voids are seen in the 0.5 wt% carbon fiber specimen, and in Figure 18B, despite a higher magnification, the 0.25 wt% carbon fiber specimen exhibits a smaller number of voids.

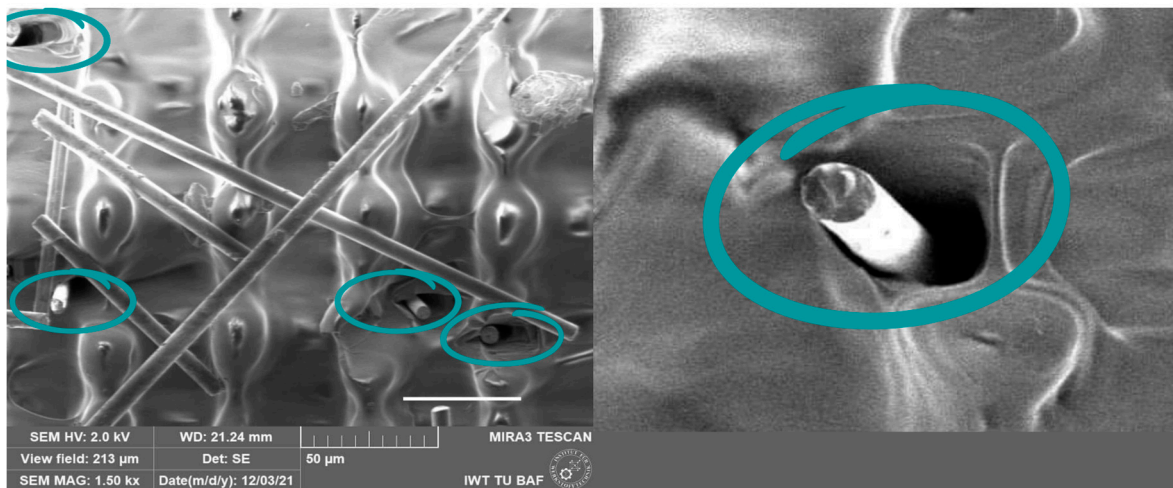
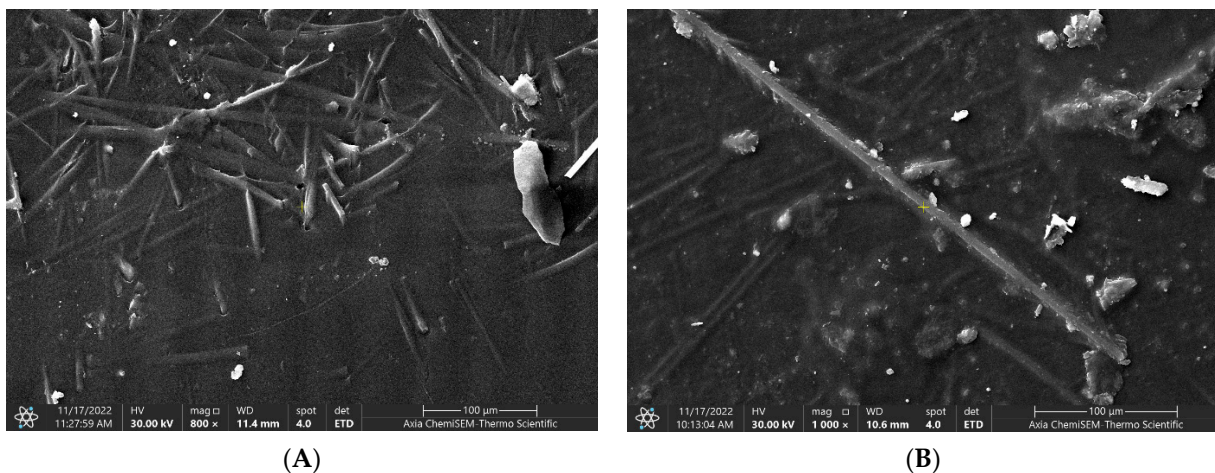


Figure 17. Voids and cracks inside the specimen in addition to the non-uniform distribution of the carbon fiber for a specimen with 0.5 wt% carbon fiber at 1.5 kx magnification using an SEM.



(A)

(B)

Figure 18. (A) SEM of the 0.5 wt% carbon: small voids can be detected at 800× magnification; (B) SEM of the 0.25 wt% carbon fiber specimen at 1000× magnification: less voids are detected due to lower carbon percentage.

4. Conclusions

This study examines the design of a technique, which may be utilised in 3D printing discontinuous fibers (i.e., milled carbon fiber) by applying SLA-like resin printing technology (LCD). SEM analyses of the 3D-printed specimens indicated that the carbon fiber was spread inside the photopolymer resin to the extent that the bottom of the object contained more carbon fiber than the top. Employing up to 2 wt% carbon fiber in 3D fabrication is possible using LCD. Tensile strength tests on the carbon fiber specimen showed that the tensile strength was enhanced with the increasing percentage of carbon fiber up to 0.25 wt%, whilst the fracture strain dropped. The printer is capable of printing with up to 2 wt% carbon fiber; however, the resulting tensile strength eventually becomes substantially lower than the sample produced with only the photopolymer resin and the fracture strain of the photopolymer resin alone is much higher than with the addition of carbon fiber. Adding 0.25 wt% carbon fiber to a 30-micrometre printing layer can boost tensile strength by 47.82%. These results should aid in the design of structural 3D-printed composite components. However, any addition of carbon fibre above 0.25 wt% causes a decrease in tensile strength, and SEM results indicate that the more carbon fiber is added, the more voids and cracks are produced.

Author Contributions: Conceptualization, R.M.S., A.K., H.Z. and R.A.; methodology, R.M.S., A.K., H.Z. and R.A.; software, R.M.S. and A.K.; validation, R.M.S. and A.K.; formal analysis, R.M.S., A.K. and R.A.; investigation, R.M.S. and A.K.; resources, A.K.; data curation, R.M.S. and A.K.; writing—original draft preparation, R.M.S.; writing—review and editing, A.K.; visualization, R.M.S. and A.K.; supervision, A.K.; project administration, H.Z.; funding acquisition, A.K. and H.Z. All authors have read and agreed to the published version of the manuscript.

Funding: The Federal Foreign Office (Auswärtiges Amt) of Germany provided funding for this study through the German Academic Exchange Service (DAAD) within the scope of the project Education and Skills in Additive Manufacturing (ESAM).

Data Availability Statement: The data presented in this study are available on request from the corresponding author.

Acknowledgments: The authors acknowledge the staff of the Chair of Additive Manufacturing (Institut für Maschinenelemente, Konstruktion und Fertigung) of TU Bergakademie Freiberg, Germany for valuable insights into the design of the experiment, mechanical testing, and technical support, as well as Heidi Engelhardt for her support in experimental planning. We also thank Anja Weidner for the SEM analyses.

Conflicts of Interest: The authors declare no conflict of interest.

References

1. Steenhuis, H.-J.; Fang, X.; Ulusemre, T. Global Diffusion of Innovation during the Fourth Industrial Revolution: The Case of Additive Manufacturing or 3D Printing. *Int. J. Innov. Technol. Manag.* **2020**, *17*, 2050005. [\[CrossRef\]](#)
2. Spencer, O.O.; Yusuf, O.T.; Tofade, T.C. Additive Manufacturing Technology Development: A Trajectory towards Industrial Revolution. *Am. J. Mech. Ind. Eng.* **2018**, *3*, 80.
3. Ngo, T.D.; Kashani, A.; Imbalzano, G.; Nguyen, K.T.Q.; Hui, D. Additive manufacturing (3D printing): A review of materials, methods, applications and challenges. *Compos. Part B Eng.* **2018**, *143*, 172–196. [\[CrossRef\]](#)
4. Kumar, S.; Kruth, J.-P. Composites by rapid prototyping technology. *Mater. Des.* **2009**, *31*, 850–856. [\[CrossRef\]](#)
5. Razavykia, A.; Brusa, E.; Delprete, C.; Yavari, R. An Overview of Additive Manufacturing Technologies—A Review to Technical Synthesis in Numerical Study of Selective Laser Melting. *Materials* **2020**, *13*, 3895. [\[CrossRef\]](#)
6. Fu, Y.F.; Rolfe, B.; Chiu, L.N.; Wang, Y.; Huang, X.; Ghabraie, K. Design and experimental validation of self-supporting topologies for additive manufacturing. *Virtual Phys. Prototyp.* **2019**, *14*, 382–394. [\[CrossRef\]](#)
7. Fu, S. Effects of Fiber Length and Fiber Orientation Distributions on the Tensile Strength of Short-fiber-reinforced Polymers. *Compos. Sci. Technol.* **1996**, *56*, 1179–1190. [\[CrossRef\]](#)
8. Blanco, I. The Rediscovery of POSS: A Molecule Rather than a Filler. *Polymers* **2018**, *10*, 904. [\[CrossRef\]](#)
9. El Moumen, A.; Tarfaoui, M.; Lafdi, K. Additive manufacturing of polymer composites: Processing and modeling approaches. *Compos. Part B Eng.* **2019**, *171*, 166–182. [\[CrossRef\]](#)
10. Blok, L.G.; Longana, M.L.; Yu, H.; Woods, B.K.S. An investigation into 3D printing of fiber reinforced thermoplastic composites. *Addit. Manuf.* **2018**, *22*, 176–186.
11. Kabir, S.M.F.; Mathur, K.; Seyam, A.F.M. A critical review on 3D printed continuous fiber-reinforced composites: History, mechanism, materials and properties. *Compos. Struct.* **2020**, *232*, 111476. [\[CrossRef\]](#)
12. Naranjo-Lozada, J.; Ahuett-Garza, H.; Orta-Castañón, P.; Verbeeten, W.M.H.; Sáiz-González, D. Tensile properties and failure behavior of chopped and continuous carbon fiber composites produced by additive manufacturing. *Addit. Manuf.* **2019**, *26*, 227–241. [\[CrossRef\]](#)
13. Shahrubudin, N.; Lee, T.; Ramlan, R. An Overview on 3D Printing Technology: Technological, Materials, and Applications. *Procedia Manuf.* **2019**, *35*, 1286–1296. [\[CrossRef\]](#)
14. Zindani, D.; Kumar, K. An insight into additive manufacturing of fiber reinforced polymer composite. *Int. J. Lightweight Mater. Manuf.* **2019**, *2*, 267–278. [\[CrossRef\]](#)
15. Parandoush, P.; Lin, D. A review on additive manufacturing of polymer-fiber composites. *Compos. Struct.* **2017**, *182*, 36–53. [\[CrossRef\]](#)
16. Kumar, S.; Hofmann, M.; Steinmann, B.; Foster, E.J.; Weder, C. Reinforcement of stereolithographic resins for rapid prototyping with cellulose nanocrystals. *ACS Appl. Mater. Interfaces* **2012**, *4*, 5399–5407. [\[CrossRef\]](#)
17. Chiu, S.-H.; Wicaksono, S.T.; Chen, K.-T.; Chen, C.-Y.; Pong, S.-H. Mechanical and thermal properties of photopolymer/CB (carbon black) nanocomposite for rapid prototyping. *Rapid Prototyp. J.* **2015**, *21*, 262–269. [\[CrossRef\]](#)
18. Compton, B.G.; Lewis, J.A. 3D-printing of lightweight cellular composites. *Adv. Mater.* **2014**, *26*, 5930–5935. [\[CrossRef\]](#)
19. Bhaskar, R.; Butt, J.; Shirvani, H. Investigating the Properties of ABS-Based Plastic Composites Manufactured by Composite Plastic Manufacturing. *J. Manuf. Mater. Process.* **2022**, *6*, 163. [\[CrossRef\]](#)
20. Park, S.; Shou, W.; Makatura, L.; Matusik, W.; Fu, K.K. 3D Printing of Polymer Composites: Materials, Processes, and Applications. *Matter* **2022**, *5*, 43–76. [\[CrossRef\]](#)

21. Dul, S.; Fambri, L.; Pegoretti, A. Fused deposition modelling with ABS-graphene nanocomposites. *Compos. Part A* **2016**, *85*, 181–191. [[CrossRef](#)]
22. Kidalov, S.; Voznyakovskii, A.; Vozniakovskii, A.; Titova, S.; Auchynnika, Y. The Effect of Few-Layer Graphene on the Complex of Hardness, Strength, and Thermo Physical Properties of Polymer Composite Materials Produced by Digital Light Processing (DLP) 3D Printing. *Materials* **2023**, *16*, 1157. [[CrossRef](#)] [[PubMed](#)]
23. Matsuzaki, R.; Ueda, M.; Namiki, M.; Jeong, T.-K.; Asahara, H.; Horiguchi, K.; Nakamura, T.; Todoroki, A.; Hirano, Y. Three-dimensional printing of continuous-fiber composites by in-nozzle impregnation. *Sci. Rep.* **2016**, *6*, 23058. [[CrossRef](#)]
24. Badanova, N.; Perveen, A.; Talamona, D. Study of SLA Printing Parameters Affecting the Dimensional Accuracy of the Pattern and Casting in Rapid Investment Casting. *J. Manuf. Mater. Process.* **2022**, *6*, 109. [[CrossRef](#)]
25. Baek, D.-M.; Park, J.-K.; Son, S.-A.; Ko, C.-C.; Garcia-Godoy, F.; Kim, H.-I.; Kwon, Y.H. Mechanical properties of composite resins light-cured using a blue DPSS laser. *Lasers Med. Sci.* **2013**, *28*, 597–604. [[CrossRef](#)]
26. Dawan, F.; Givens, M.; Williams, L.; Mensah, P. Carbonated 3D-Printable Polymer Composite for Thermo-Mechanically Stable Applications. *J. Manuf. Mater. Process.* **2022**, *6*, 66. [[CrossRef](#)]
27. Sugiyama, K.; Matsuzaki, R.; Ueda, M.; Todoroki, A.; Hirano, Y. 3D printing of composite sandwich structures using continuous carbon fiber and fiber tension. *Compos. Part A* **2018**, *113*, 114–121. [[CrossRef](#)]
28. Brosh, T.; Ganor, Y.; Belov, I.; Pilo, R. Analysis of strength properties of light-cured resin composites. *Dent. Mater.* **1999**, *15*, 174–179. [[CrossRef](#)]
29. Kalia, S.; Kaith, B.S.; Kaur, I. Pretreatments of natural fibers and their application as reinforcing material in polymer composites—A review. *Polym. Eng. Sci.* **2013**, *49*, 1253–1272. [[CrossRef](#)]
30. Karalekas, D.E. Study of the mechanical properties of nonwoven fibre mat reinforced photopolymers used in rapid prototyping. *Mater. Des.* **2003**, *24*, 665–670. [[CrossRef](#)]
31. Tekinalp, H.L.; Kunc, V.; Velez-Garcia, G.M.; Duty, C.E.; Love, L.J.; Naskar, A.K.; Blue, C.A.; Ozcan, S. Highly oriented carbon fiber-polymer composites via additive manufacturing. *Compos. Sci. Technol.* **2014**, *105*, 144–150. [[CrossRef](#)]
32. Ning, F.; Cong, W.; Qiu, J.; Wei, J.; Wang, S. Additive manufacturing of carbon fiber reinforced thermoplastic composites using fused deposition modeling. *Compos. Part B Eng.* **2015**, *80*, 369–378. [[CrossRef](#)]
33. Rahman, A.; Islam, Z.; Gibbon, L.; Ulven, C.A.; La Scala, J.J. 3D Printing of Continuous Carbon Fiber Reinforced Thermoset Composites Using UV Curable Resin. *Polym. Compos.* **2021**, *42*, 5859–5868. [[CrossRef](#)]
34. Shinde, V.V.; Wang, Y.; Salek, M.F.; Auad, M.L.; Beckingham, L.E.; Beckingham, B.S. Material Design for Enhancing Properties of 3D Printed Polymer Composites for Target Applications. *Technologies* **2022**, *10*, 45. [[CrossRef](#)]
35. Yunus, D.E.; He, R.; Shi, W.; Kaya, O.; Liu, Y. Short fiber reinforced 3d printed ceramic composite with shear induced alignment. *Ceram. Int.* **2017**, *43*, 11766–11772. [[CrossRef](#)]
36. Wang, X.; Jiang, M.; Zhou, Z.; Gou, J.; Hui, D. 3D printing of polymer matrix composites: A review and prospective. *Compos. Part B Eng.* **2017**, *110*, 442–458. [[CrossRef](#)]
37. Dickson, A.N.; Abourayana, H.M.; Dowling, D.P. 3D Printing of Fibre-Reinforced Thermoplastic Composites Using Fused Filament Fabrication—A Review. *Polymers* **2020**, *12*, 2188. [[CrossRef](#)] [[PubMed](#)]
38. Jahangir, M.; Billah, K.; Lin, Y.; Roberson, D.; Wicker, R.; Espalin, D. Reinforcement of material extrusion 3D printed polycarbonate using continuous carbon fiber. *Addit. Manuf.* **2019**, *28*, 354–364. [[CrossRef](#)]
39. Yeong, W.Y.; Goh, G.D. 3D Printing of Carbon Fiber Composite: The Future of Composite Industry? *Matter* **2020**, *2*, 1361–1363. [[CrossRef](#)]
40. ELEGOO Official. ELEGOO ABS-Like LCD UV-Curing Photopolymer Rapid Resin for 3D Printers. Available online: www.elegoo.com/products/elegoo-abs-like-resin (accessed on 20 August 2022).
41. Aniwaa. List of 3D Printing Technologies—Guide on All 3D Printing Technologies. 5 August 2021. Available online: www.aniwaa.com/guide/3d-printers/3d-printing-technologies (accessed on 8 December 2022).
42. Hwang, S.R.; Park, M.S. Property Analysis of Photo-Polymerization-Type 3D-Printed Structures Based on Multi-Composite Materials. *Appl. Sci.* **2021**, *11*, 8545. [[CrossRef](#)]
43. Guo, H.; Lv, R.; Bai, S. Recent Advances on 3D Printing Graphene-based Composites. *Nano Mater. Sci.* **2019**, *1*, 101–115. [[CrossRef](#)]
44. Sano, Y.; Matsuzaki, R.; Ueda, M.; Todoroki, A.; Hirano, Y. 3D printing of discontinuous and continuous fibre composites using stereolithography. *Addit. Manuf.* **2018**, *24*, 521–527. [[CrossRef](#)]
45. Barad, M. Design of Experiments (DOE)—A Valuable Multi-Purpose Methodology. *Appl. Math.* **2014**, *5*, 48158. [[CrossRef](#)]
46. *ASTM D638-14*; Standard Test Method for Tensile Properties of Plastics. ASTM International: West Conshohocken, PA, USA, 2015.
47. *ASTM F2792-12a*; Standard Terminology for Additive Manufacturing Technologies. ASTM International: West Conshohocken, PA, USA, 2013; pp. 10–12.
48. Tumbleston, J.R.; Shrivanyants, D.; Ermoshkin, N.; Januszewicz, R.; Johnson, A.R.; Kelly, D.; Chen, K.; Pinschmidt, R.; Rolland, J.P.; Ermoshkin, A.; et al. Continuous liquid interface production of 3D objects. *Science* **2015**, *347*, 1349–1352. [[CrossRef](#)]

Disclaimer/Publisher’s Note: The statements, opinions and data contained in all publications are solely those of the individual author(s) and contributor(s) and not of MDPI and/or the editor(s). MDPI and/or the editor(s) disclaim responsibility for any injury to people or property resulting from any ideas, methods, instructions or products referred to in the content.